

RESEARCH ARTICLE

Performance of enhanced modal participation ratio in multiple-story damage localization

Zafer Yılmaz^{1*}, Murat Günaydın², Fatih Yesevi Okur², Ertugrul Taciroglu¹

- ¹ UCLA Samueli School of Engineering, Civil and Environmental Engineering, Los Angeles, CA, USA
- ¹ Karadeniz Technical University, Department of Civil Engineering, Trabzon, Türkiye

Article History

Received 20 June 2025 Accepted 10 July 2025

Keywords

Damage localization
Enhanced modal participation
ratio
Ambient vibration test
Dynamic characteristics
Modal analysis

Abstract

This study evaluates the effectiveness of the Modal Participation Ratio (MPR) and Enhanced Modal Participation Ratio (EMPR) methods for damage localization, specifically in multi-story structures with combined story damage scenarios. The originality of this work lies in its combined use of numerical and experimental validation on the same four-story steel frame model, focusing on complex multidamage conditions rather than single-story or simulation-only studies. MPR values were derived from dynamic responses of a finite element model of a steel frame, obtained through numerical simulations using randomized white noise acceleration, while EMPR values were derived from experimental tests conducted on the same steel frame model, utilizing ambient vibrations. Thirteen damage scenarios, including single-, two-, and three-story combinations, were investigated. The results show that damaged degrees of freedom consistently exhibit the highest ΔMPR values, and that combined damage scenarios often produce additive MPR patterns that aid in damage separation. First-story damage had the most dominant effect on overall MPR variation, occasionally reducing the visibility of higher-story damage. The findings confirm that both methods are reliable tools for structural health monitoring and damage identification, even in complex multi-damage configurations.

1. Introduction

Monitoring the changes in the structure's health presents an opportunity to detect any adverse developments that might cause economic loss or, worse, loss of lives. Researchers focusing on structural health monitoring aim to develop or enhance methods to identify structural systems or damage/damage propagation. While coming up with an idea of a method takes much effort, testing these methods for their effectiveness and coming up with solutions to eliminate these defects is as essential as developing a new method. One of the most used methods of identifying structure or damage is studying dynamic characteristics such as natural frequency, mode shape, and damping ratio. These characteristics can be obtained through non-destructive tests or monitored for any change. A change signaling that the building went under internal or external forces, which resulted in a loss of strength.

^{*} Corresponding author (zafer@ucla.edu)

Many studies were conducted to test natural frequency, mode shape, damping ratio, and many more dynamic characteristics. The significant steps of damage identification through these characteristics are detection, localization, and damage quantification. While one can assume that the structure is damaged after observing a change in these dynamic characteristics, localizing and quantifying the damage is more challenging. Many ways of evaluating the effectiveness of damage identification methods have been carried out numerically and experimentally. For instance, a damaged member, the number of damaged members, the distance between damaged members, and the quantity of damage on all damaged members can be diversified to assess the effectiveness of the presented method.

The localization of damage has been one of the main challenges for complex structures and single system members. There have been various methods developed and evaluated for damage localization on beam-type structures, plate-like structures, trusses, and 3-D frame structures [2-5,9,11-13,16,17,19,23,24,30,34-36,38,42,43]. While predicting the existence of damage and its location is a challenge, having multiple damage locations makes it even more difficult to predict. Therefore, multiple damage localization is a milestone for newly developed methods. Contursi et al. [15] developed a new method for multiple damage localization in elastic structures using a two-bar truss, a fifteen-bar truss, and a ten-bay, 51-bar truss. The method was defined as attractive for practice for the reason of only requires knowledge of natural frequency changes in the structure. Lu et al. [25] studied two methods for multiple damage localization in beam structures. The first method is to study the sensitivity of flexibility and flexibility curvature to various damage patterns performed on the FE model. And the second method, which was found to be more effective, where relative frequency changes in the multiple damage location assurance criterion (MDLAC). Xiang and Liang [37] developed a two-step approach for multiple damage detection in thin plates. The method consists of the application of a 2D wavelet to the modal shape for the detection of singularity and damage location, followed by a particle swarm optimization algorithm to further assess these outcomes. Papers focused on developing or testing multiple damage localization on several types of structures and members can be found in the literature [10,18,21,22,26,28,29,32,33].

Modal Participation Ratio (MPR) is a representative contribution value of each considered mode and each considered measurement point or degree of freedom (DOF) to the modal behavior of the examined structure. And evaluating changes on these ratios provides a good source for damage identification. The study by Yilmaz et al. [40] introduced and experimentally validated the enhanced MPR approach for single-story damage scenarios, demonstrating that the version filtered using MAC-based rejection was more effective than MPR values derived using bandpass filtering. This study is a direct continuation of that work and evaluates the effectiveness of the proposed enhanced MPR as a multiple damage localization parameter, extending its use to combined damage cases. Using the same multi-story steel frame model, changes in MPR through single and multi-story damage scenarios have been numerically and experimentally studied. As the first study to experimentally examine MPR under multiple damage scenarios, it provides evidence that, in most cases, MPR changes are sensitive enough to identify new damage locations, supporting the method's potential for real-world structural health monitoring applications.

2. Building model

A simple steel frame model simulating the dynamic behavior of a building is constructed using a rectangular hollow section (40×40×2 mm). The dimensions of the model used for experimental and numerical tests are provided in Fig. 1. As shown in Fig. 1, the model consists of a frame and a base plate welded to the frame. Eight holes in the base plate are used to secure the model to the ground, simulating fixed boundary conditions.

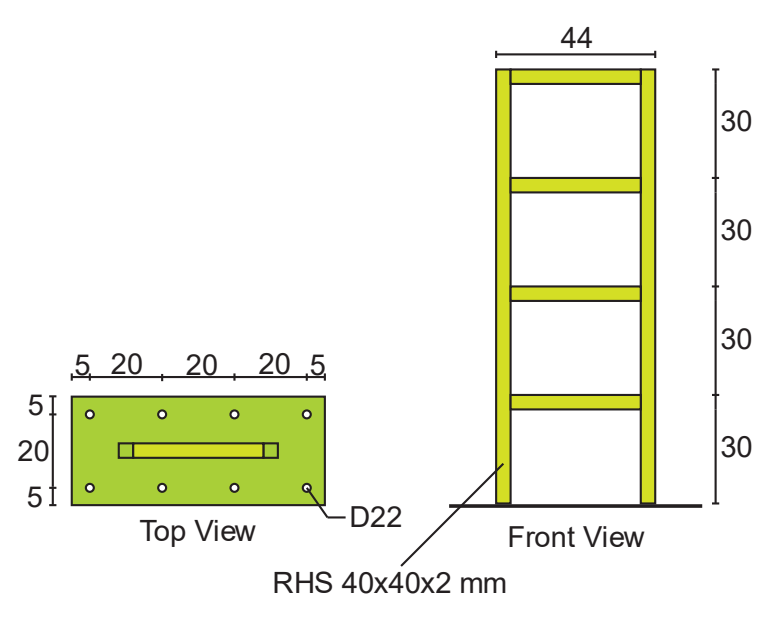


Fig. 1. The frame model and base plate (dimensions in cm)

3. Methodology

The methodology for obtaining MPR can be divided into two phases: dynamic response extraction and MPR formulation. Dynamic response extraction approaches are presented in Fig. 2. A numerical approach to achieving a dynamic response involves employing transient analysis, where artificial vibrations simulate ambient vibrations caused by environmental effects in a numerical model of a building. These dynamic responses are collected by applying randomized white noise acceleration as ambient excitations. Determining the appropriate time step and total duration of white noise acceleration is crucial for accurate modal response, with considerations based on the studied frequency range [20]. Dynamic responses of building models are acquired by utilizing Operational Modal Analysis (OMA). Accelerometers are employed to measure the dynamic response of objects. No artificial vibrations are required since the ambient vibrations created by the environment are enough to create dynamic excitation. Then, these responses measured by accelerometers are collected and stored in data acquisition systems. Later, these dynamic responses can be used to obtain dynamic characteristics like natural frequency, mode shapes, and damping ratios. The Enhanced Frequency Domain Decomposition (EFDD) method is employed to extract these dynamic characteristics [6].

MPR derivation involves utilizing dynamic responses. Different MPR values can be obtained depending on the dynamic response type. This study employs acceleration responses obtained from transient analysis and OMA. Unlike the modal participation mass ratio, MPR quantifies the contribution of each measurement point or DOF to each mode, allowing more precise structural damage detection between measurement points or DOFs. Fig. 3 shows the step-by-step derivation of the MPR formulation. As the first step, the Fast Fourier Transform (FFT) procedure is employed to convert the dynamic response of a single measurement point to frequency domain data. Then, filtering is applied to separate the frequency domain data of a single measurement point into considered modes.

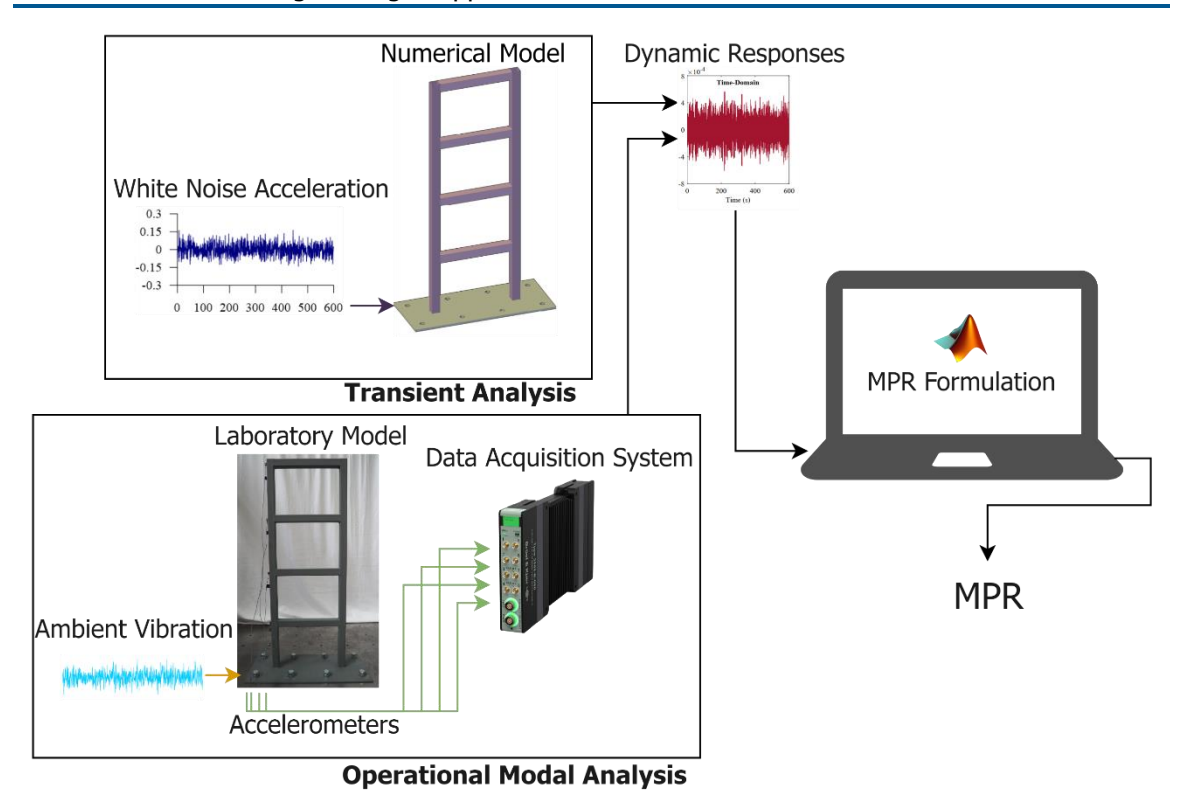


Fig. 2. Dynamic response extraction flowchart for numerical and experimental models

In this study, the first three mode shapes are selected for MPR derivation. These modes were chosen because they contribute most significantly to the global dynamic behavior of the four-story frame model. Higher modes were excluded due to their lower energy content and higher sensitivity to noise, especially in experimental measurements. This selection ensures a balance between sensitivity to damage and reliability of results.

MAC rejection filtering, which enhances the accuracy of damage localization by evaluating the correlation between mode shapes, has proven to have better results in experimental studies and is utilized in experimental studies. In this study, a MAC rejection level of 0.9 is selected. This level provides the lower and upper frequency bounds for each mode frequency, defining the frequency range where the mode shapes have higher relevance. These bounds are then used in subsequent steps of the methodology, as outlined in [40]. In contrast, bandpass filtering with a user-defined value of 1 is utilized for the numerical study [27]. The third step is to apply the inverse FFT to obtain a modal response for a single mode. Then, the root square of this modal response is calculated in step four. Step five is repeating steps three and four for each considered mode. The procedure from steps one to five is repeated for the dynamic response of each measurement point in step six. At the end of the sixth step, the root mean square of each mode for each measurement point is derived. In step seven, the MPR is determined by calculating the ratio of the root mean square of each modal response to the sum of all considered modal responses. The damage identification procedure involves assessing the percentage change in MPR values between damaged and initial states. Therefore, step eight is repeating all the steps for each structural state. Lastly, in step nine, MPR variation is studied for damage identification, where the percentage change of damaged MPR (DMPR) to initial MPR (IMPR) is derived.

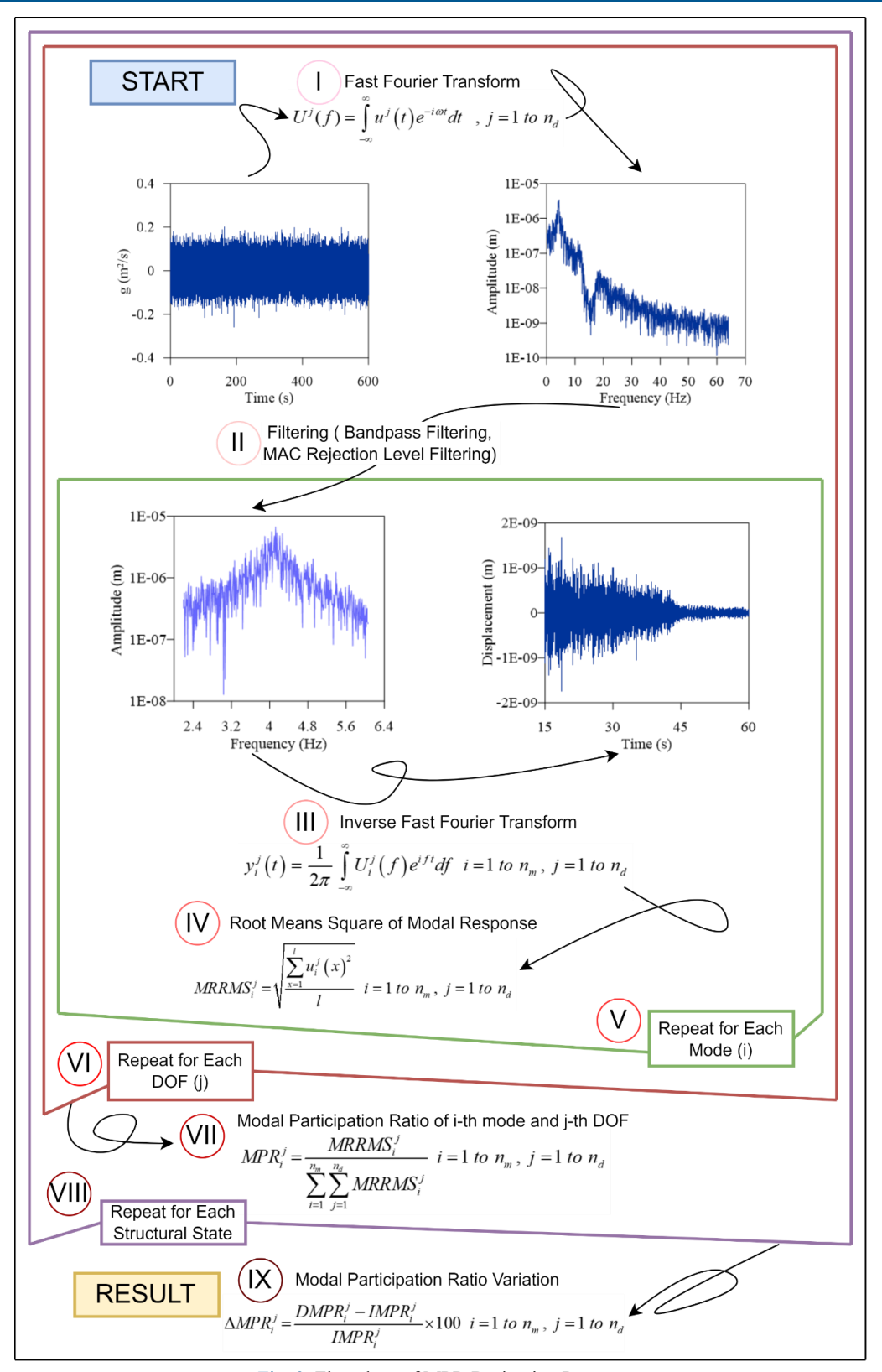


Fig. 3. Flowchart of MPR Derivation Process

4. Damage scenarios

In addition to undamaged and single-story damage scenarios completed in Yilmaz et al. [40], multi-damage scenarios were studied in numerical and experimental tests. Fig. 4 shows all damage scenarios that were considered in this study.

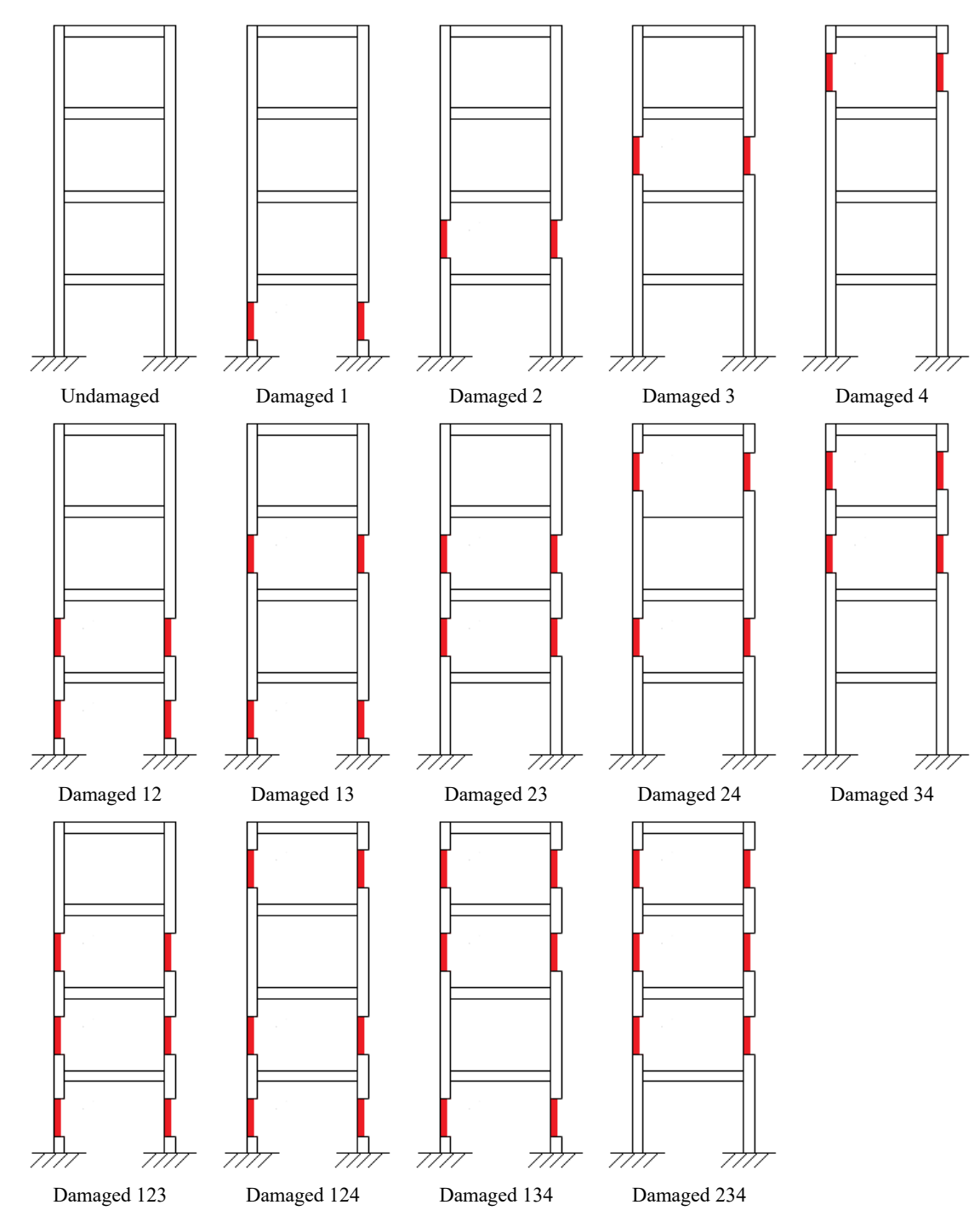


Fig. 4. Illustration of damage scenarios applied to the model



Fig. 5. Multiple damage building models

The selected damage scenarios include both adjacent and non-adjacent multi-story damage combinations to reflect varying levels of localization complexity and simulate realistic structural damage patterns that may occur during seismic or progressive deterioration events. This approach allows a more thorough evaluation of MPR's performance under different conditions.

Story damage was simulated as removing a part with 140mm height and 20mm width from the middle of the story. These scenarios were employed to evaluate the multiple damage localization performance of MPR in damage identification. Multiple damage building models are given in Fig. 5.

5. Numerical study

A numerical study has been performed to confirm that the same behavior of MPR change can be observed in both experimental and numerical studies. Thus, expanding the application area of the method. The results of the numerical study are also utilized to help verify experimental results. The finite element (FE) model of the steel frame is built and tested on SAP2000 software (CSI, 2021). In addition to transient analysis, which gives dynamic responses used in MPR derivation, modal analysis was carried out to obtain dynamic characteristics of the model, such as natural frequencies and mode shapes. The first three in-plane mode natural frequencies of all structural states are given in Table 1. The undamaged state's first, second, and third mode frequencies are 65.248, 227.732, and 458.989 Hz, respectively. All structural states' first, second, and third mode frequencies are between 54.579 and 66.839Hz, 180.957 and 227.732Hz, and 341.232 and 458.989Hz, respectively. The comparison of the first mode frequency of models with and without fourth-story damage shows a clear indication of an increase in frequency when fourth-story damage is introduced. This behavior might be misleading when the damage localization is not backed by other parameters.

Fig. 6 shows the frequency variation of the first mode frequency for each damage state. There is a decrease in first-mode natural frequencies except for the third and fourth-story combined damage scenario and the single fourth-story damage scenario. The first and second-story damage combination resulted in the highest decrease in the first mode frequency value of 16.35%. Moreover, the highest decrease in single-story damage scenarios is first-story damage, with a 14.52% decrease in first-mode frequency. All six damage scenarios that include first-story damage caused the most decrease in the first mode natural frequency. Lower story damages have a higher impact on the first mode frequency.

The mode shapes obtained from numerical modal analysis and a close look at each eigenvector of each damage state for the first three translational modes are presented in Fig. 7. These mode shapes are weighted and normalized to an undamaged structural state.

Studying eigenvalues and eigenvectors was one of the first damage identification methods developed [1, 31, 41]. A detailed study of the relation of these values to damage location can provide a reasonable estimate.

However, MPR value variation, once derived, gives a simple indication of damage location and quantity. First-mode MPR variations caused by single-story and multi-story damage scenarios are calculated using a bandpass filter and MAC rejection filter [27,40]. The user-defined filtering value was assumed to be one, and the MAC rejection level was 0.9. However, both methods gave the same MPR variation results, meaning the filtering interval does not affect MPR variation in the case of the numerical study. Fig. 8 shows MPR variations (Δ MPR) for all single-story and combined-story damage scenarios. The Δ MPR value of damaged DOF was the highest among all other MPR variations. For single-story damage scenarios, the highest increase in MPR occurred at the damaged-story DOF. For combined damage scenarios, the highest increase was at one of the damaged DOFs. In the damage scenarios with first-story damage, the Δ MPR of the first DOF has an apparent increase.

Table 1. Natural frequencies of FE models and frequency variations

| Structural State | First Mode Frequency (Hz) | Second Mode Frequency (Hz) | Third Mode Frequency (Hz) |
|------------------|------------------------------|-------------------------------|---------------------------|
| Undamaged | 65.248 | 227.732 | 458.989 |
| Damage 1 | 55.776 | 200.864 | 421.78 |
| Damage 2 | 62.666 | 221.288 | 399.393 |
| Damage 3 | 65.048 | 206.9 | 446.798 |
| Damage 4 | 66.839 | 217.989 | 404.473 |
| Damage 12 | 54.579 | 196.589 | 372.594 |
| Damage 13 | 55.982 | 184.206 | 419.406 |
| Damage 23 | 62.644 | 205.360 | 393.405 |
| Damage 24 | 64.270 | 213.282 | 364.839 |
| Damage 34 | 66.792 | 201.342 | 392.454 |
| Damage 123 | 54.873 | 183.646 | 368.005 |
| Damage 124 | 55.957 | 192.071 | 341.232 |
| Damage 134 | 57.449 | 180.957 | 374.926 |
| Damage 234 | 64.397 | 200.354 | 362.225 |

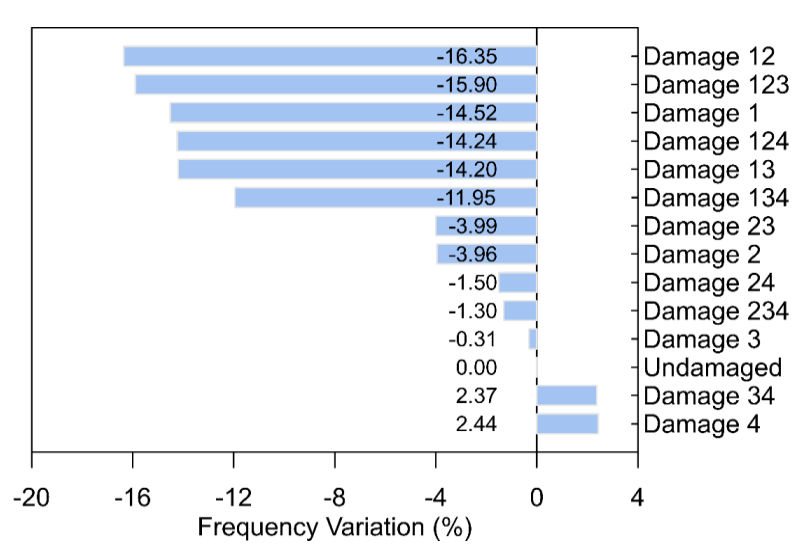


Fig. 6. The first mode frequency variation of FE models

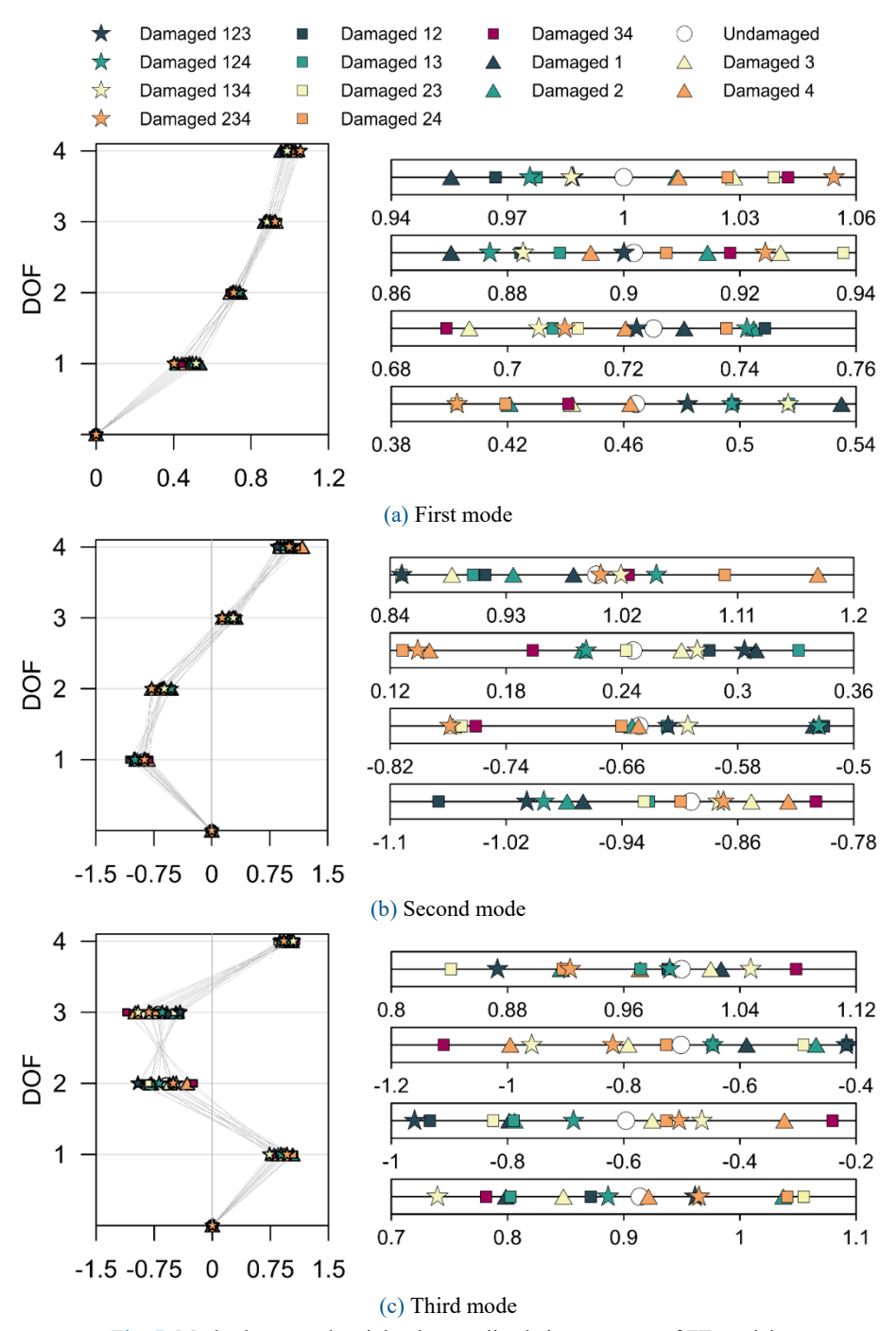


Fig. 7. Mode shapes and weighted normalized eigen vectors of FE models

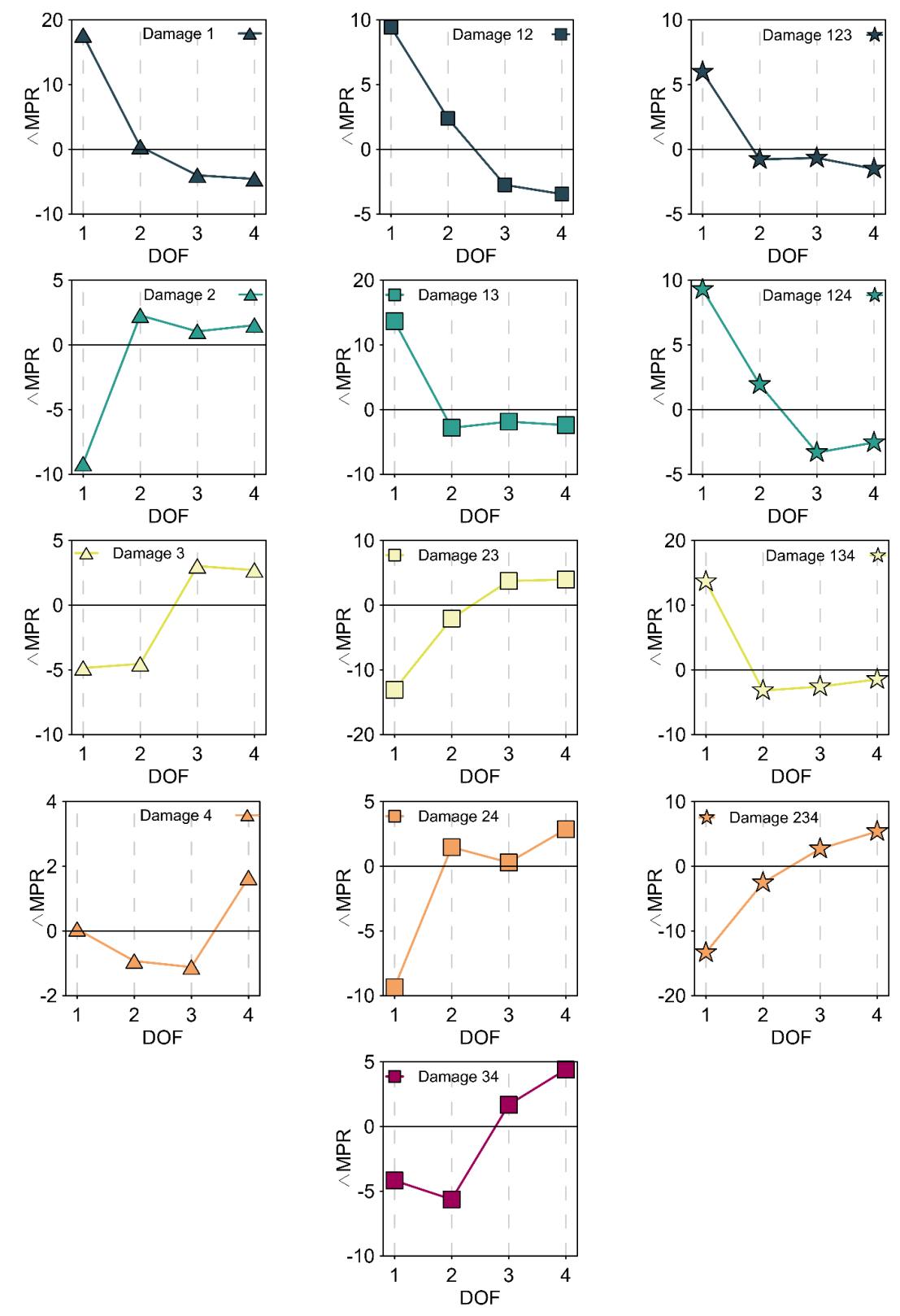


Fig. 8. MPR Variations of FE models for all damage states

On the contrary, in combined damage scenarios with fourth-story damage, Δ MPR for the fourth DOF shows a minor impact on all MPR values. Therefore, it is easier to interpret the involvement of first-story damage compared to fourth-story damage. However, two- and three-story combination damage scenarios create MPR variation, which is approximately a simple summation of single-story damage scenarios that provide a straightforward damage localization practice. For instance, Damage 13 case, where the building model is damaged on the first and third stories, shows a combined MPR variation of first and third-story damages. Since the first story damage is more dominant on MPR variations, it is still differentiable in Damage 13. The third story damage in Damage13 can also be spotted because it has the second-highest MPR variation. Moreover, Damage 13, compared to Damage 1, shows signs of additional third-story damage. The same approach can be applied to other multiple-story damage scenarios. Consequently, it shows that combined damage scenarios can be interpreted through MPR changes.

6. Experimental study

The dynamic responses of the building models are collected as part of OMA. This method requires the utilization of a measurement setup, data acquisition, and processing of data. B&K 4507-type uni-axial accelerometers and uni-axial signal cables have been used to measure and transfer data to the B&K 3053 data acquisition system. Then, the data was processed using the BK Connect (2021) software. The dynamic responses collected were the excitation of the model to ambient vibrations. Ten minutes of dynamic response readings were recorded for each case. The accelerometer used has a sensitivity of 1 V/g and an operational frequency range of 0.4–6000 Hz. The accelerometers were placed on the models in the longitudinal direction to measure in-plane dynamic responses (Fig. 9). The Nyquist frequency was set to 2048 Hz for the experimental study, which was enough to observe the first three translational modes. Each model's dynamic characteristics, such as natural frequency, mode shape, and damping ratio, were obtained using OMA software [7, 8]. More information about the experimental setup and equipment is presented in [39].

The natural frequencies and damping ratios of all damage states obtained with EFDD are presented in Table 2. The undamaged state's first, second, and third mode frequencies are 67.958, 231.753, and 459.544 Hz, respectively. These modes also have 2.943, 0.972, and 0.505% damping ratios, respectively. All structural states' first, second, and third mode frequencies are between 53.996 and 68.059, 172.363 and 231.753Hz, and 284.11 and 549.544Hz, respectively. Damping ratios of the first three translational modes vary between 2.897 and 4.295%, 0.936 and 1.303%, and 0.505 and 1.152%, respectively. Similar to numerical model values, the introduction of fourth-story level damage to the model increases the mode frequency, which could lead to misinterpretation of damage location.

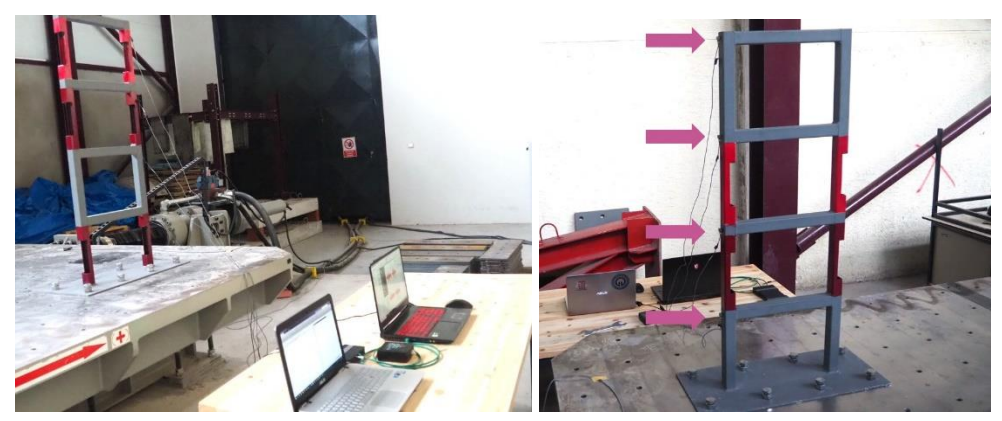


Fig. 9. The first mode frequency variation of FE models

| Structural State | First Mode | | Second | Second Mode | | Third Mode |
|------------------|----------------|----------------------|----------------|----------------------|----------------|----------------------|
| | Frequency (Hz) | Damping Ratio (%) | Frequency (Hz) | Damping Ratio (%) | Frequency (Hz) | Damping Ratio (%) |
| Undamaged | 67.958 | 2.943 | 231.753 | 0.972 | 459.544 | 0.505 |
| Damage 1 | 58.66 | 4.088 | 200.018 | 0.991 | 409.331 | 0.542 |
| Damage 2 | 59.674 | 3.715 | 224.004 | 0.936 | 377.608 | 0.625 |
| Damage 3 | 64.868 | 3.464 | 208.044 | 1.022 | 417.284 | 0.554 |
| Damage 4 | 68.059 | 2.897 | 210.393 | 1.103 | 385.829 | 0.579 |
| Damage 12 | 54.439 | 4.295 | 196.048 | 1.021 | 342.646 | 0.655 |
| Damage 13 | 55.671 | 3.869 | 172.363 | 1.235 | 382.251 | 0.626 |
| Damage 23 | 60.177 | 3.409 | 198.593 | 1.159 | 291.409 | 0.785 |
| Damage 24 | 61.198 | 3.947 | 199.663 | 1.074 | 284.11 | 0.824 |
| Damage 34 | 66.017 | 3.396 | 189.215 | 1.176 | 286.441 | 1.152 |
| Damage 123 | 53.996 | 4.242 | 179.963 | 1.109 | 337.795 | 0.664 |
| Damage 124 | 55.967 | 3.542 | 180.253 | 1.155 | 304.846 | 0.738 |
| Damage 134 | 58.727 | 3.808 | 174.861 | 1.303 | 327.957 | 0.624 |
| Damage 234 | 60.016 | 3.24 | 188.894 | 1.192 | 319.664 | 0.701 |

Table 2. Mode frequencies and damping ratios of steel frame models obtained with EFDD

Fig. 10 shows the frequency variation of the first mode frequency for each damage state. Except for the single fourth-story damage scenario, there is a decrease in first-mode natural frequencies of all damage scenarios. The first, second, and third story damage combination resulted in the highest first mode frequency value decrease of 20.55%. The highest decrease in single-story damage scenarios is first-story damage, with a 13.68% decrease in first-mode frequency. All six damage scenarios that include first-story damage caused the most decrease in first-mode natural frequency, which once again shows the high impact of first-story damage on first-mode mode frequency. Moreover, adding second-story and/or third-story damage to first-story damage caused the first mode's natural frequency to drop even more. Ultimately, lower story damages have a higher effect on the first mode natural frequency.

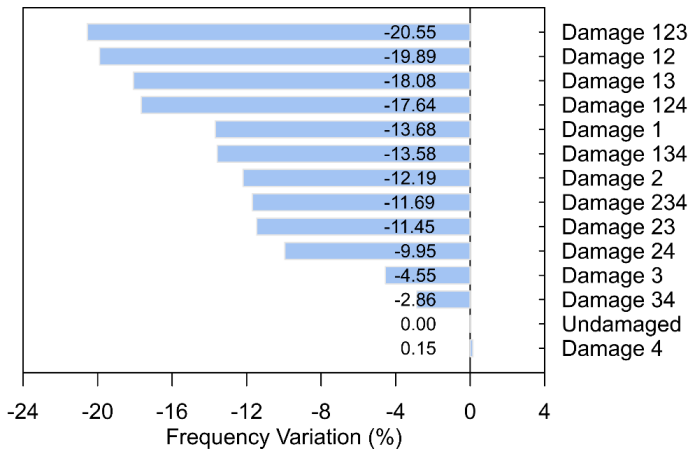


Fig. 10. The first mode frequency variation of building models

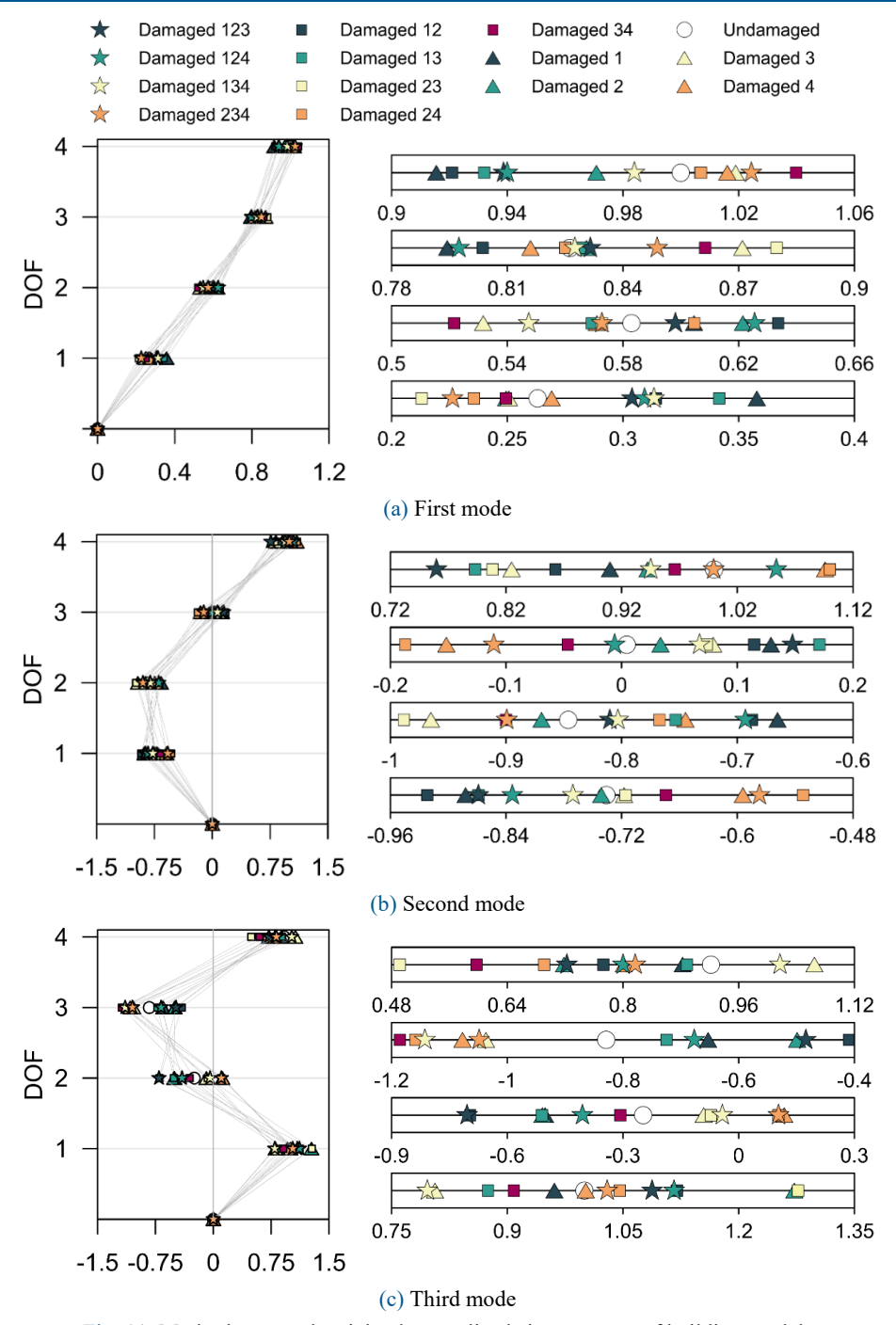


Fig. 11. Mode shapes and weighted normalized eigen vectors of building models

The mode shapes obtained from operational modal analysis and a close look at each eigenvector of each damage state for the first three translational modes are presented in Fig. 11. These mode shapes are weighted and normalized to an undamaged structural state. Damage identification through these values requires a detailed study of the relation between the damage state and each eigenvector element.

The MAC rejection level filtering method explained in Yilmaz (2023) is more effective on real-life models. Since it does not entirely depend on the user-defined gamma value used in bandpass filtering, it gives a more accurate estimation of MPR variations without a trial-and-error process. Fig. 12 shows the first and third stories' combined damage state MPR variations calculated by a 0.9 MAC rejection level, 0.5 gamma, and one gamma value. All three have indications of first-story damage. However, only MPR variations calculated using a 0.9 MAC rejection level have a more unambiguous indication of third-story damage. Decreasing the gamma factor caused the first mode MPR of the third DOF to increase; however, there is no reasoning behind selecting the gamma value without prior knowledge of damage locations.

Fig. 13 shows MPR variations for all single-story and combined-story damage scenarios. The ΔMPR value of damaged DOF was the highest among all other MPR variations. For single-story damage scenarios, the damaged DOF is visible as they have the highest increase in MPR. Two-story combined damages, except the second and third-story damage combinations, can also be interpreted by the highest increase in MPR in both damage DOFs. When comparing three-story damage combinations to two-story or single-story damage scenarios, additional damage locations can be clearly defined. For example, Damage 123, compared to Damage 12, shows an increase in the MPR value of the third DOF, indicating the occurrence of damage at this location. A combination of single-story damage scenarios can be used to foresee possible combined MPR variations and two-story damage scenarios for three-story damage scenarios. It should also be noted that first-story damage has a higher impact on total MPR variations, which might cause higher-story damage to be misinterpreted. Similarly, at high story combined damage scenarios, one can suppress the sign of having the other. For instance, comparing single third-story damage and combined third and fourth-story damage, the addition of fourth-story damage is not very salient. However, these less noticeable relationships between some of the combined damage MPR variations provide reliable sources along with mode frequency, mode shape, and damping ratio changes.

Numerical and experimental studies both show that MPR is effective in damage localization of single and multiple-story damage. These methods can be used interchangeably. However, an experimental study requires the use of an enhanced MPR proposed to obtain a better estimation of damage location. Moreover, enhanced MPR provides clearer signs of damage location in combined damage scenarios such as Damage 12, Damage 123, Damage 13, Damage 124, and Damage 134. Additionally, in case of lower story damage, possible higher story damages can be overlooked. Therefore, it is important to check mode frequency, mode shape, and damping ratios to verify the damage location. To summarize the performance of MPR across different damage scenarios, Table 3 provides a concise overview of ΔMPR patterns and localization clarity.

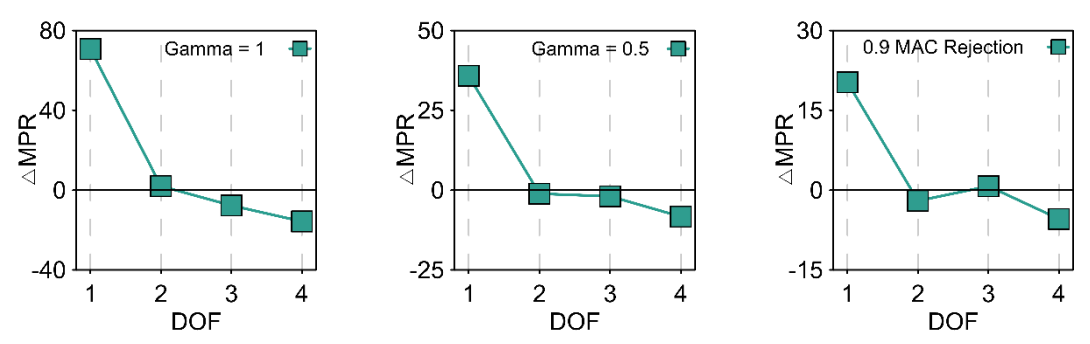


Fig. 12. Comparison of filtering methods for Damage 13 case: Bandpass and MAC rejection filtering

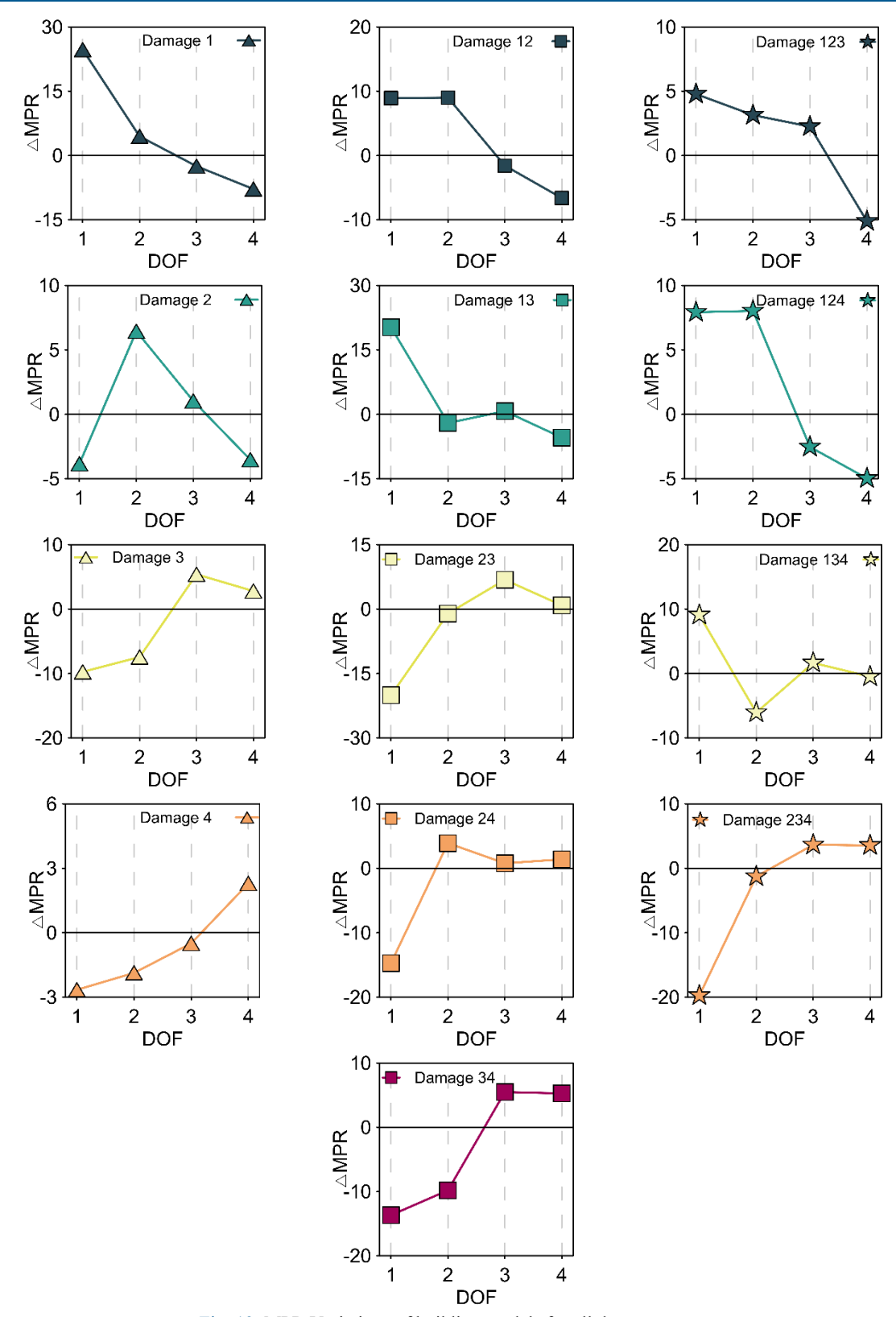


Fig. 13. MPR Variations of building models for all damage states

| Damage Scenario | ΔMPR Pattern | Localization Clarity | Notes | |
|----------------------|----------------------------|------------------------|--|--|
| Single-story | Clear peak at damaged DOF | High | Most reliable case | |
| Two-story | Peaks at both damaged DOFs | Moderate to High | First-story damage often dominates | |
| Three-story | Additional peak visible | Moderate | Some higher-story damage may be masked | |
| First-story involved | Dominant ΔMPR response | High (for first story) | Can overshadow upper-story damage | |
| Upper story only | Subtle ΔMPR changes | Low to Moderate | Harder to detect without enhancements | |

Table 3. Summary of MPR behavior across damage scenarios

7. Conclusions

The performance of MPR as a damage localization indicator was evaluated with single-story and combined-story damages. The four-story steel frame model was selected as the building model. Thirteen damage scenarios were studied numerically and experimentally. Damage occurrence caused first-mode natural frequencies to drop in both experimental and numerical studies, except for fourth-story damage in both and third and fourth-story combined damage in numerical studies. Damage scenarios, including first-story damages, resulted in a higher decrease in first-mode frequency but not in the same order for the numerical and experimental studies. The mode shapes of the model had significant changes caused by each damage scenario. Damping ratios derived from laboratory measurements show that the introduction of damage generally increases the damping ratio. However, studying these dynamic characteristics for damage identification requires a complicated process of defining relationships between the damage location and the parameter.

MPR goes through significant and visible changes based on the damage location. For single-story damages, the first-mode MPR value of damage DOF has the highest increase among all first-mode MPR values. For combined damage scenarios, the highest increase occurs in one of the damaged DOFs. In the damage scenarios with first-story damage, the ΔMPR of the first DOF has an apparent increase. On the contrary, in combined damage scenarios with fourth-story damage, ΔMPR for the fourth DOF shows a minor impact on all MPR values. Therefore, it is easier to interpret the involvement of first-story damage compared to fourth-story damage. However, two- and three-story combination damage scenarios create MPR variation, which is approximately a simple summation of single-story damage scenarios that provide a straightforward damage localization practice. A comparison of MPR variations of single-story and combined-story damage scenarios shows that new damage locations have been introduced.

Finally, based on the results of this case, it is concluded that the MPR variation was effective in both numerical and experimental damage localization of single and combined damage. It should be noted that the method requires knowledge of the initial condition of the structure because it is based on a comparative approach. While this is feasible in controlled laboratory settings, it may be impractical for many real-life structures where undamaged baseline data is not available. This limitation should be considered when applying the method in the field. Constant monitoring of buildings and MPR changes can provide insight into the structure's stiffness changes. However, environmental factors such as temperature fluctuations and operational vibrations may affect ambient response measurements and, consequently, MPR values. In future studies, higher mode MPR values can be further studied to address the uncertainty in localizing high-story damage in the presence of low-story damage. Additionally, different damage types that result in smaller

stiffness changes, such as cracking, can be examined to validate the method's precision. Different building models with non-uniform shapes can also be used to understand the behavior of MPR variations. Moreover, applying the method to full-scale structures will require addressing sensor limitations, boundary condition uncertainties, and elevated noise levels typically encountered in real-world monitoring systems.

Author contributions

Author Contributions: Conceptualization, M.G.; Software, Z.Y. and F.Y.O.; Validation, F.Y.O.; Formal analysis, Z.Y. and F.Y.O.; Writing—original draft, Z.Y. and M.G.; Writing—review & editing, E.T.; Visualization, M.G.; Supervision, E.T.; Project administration, M.G.

Declaration of conflicting interests

The author(s) declared no potential conflicts of interest with respect to the research, authorship, and/or publication of this article.

Funding

The author(s) disclosed receipt of the following financial support for the research, authorship, and/or publication of this article: This work was supported by the Karadeniz Technical University under Research Grant No. FHD-2022-10402.

Data availability statement

The datasets generated and/or analyzed during the current study are available from the corresponding author on reasonable request.

References

- [1] Adams RD, Cawley P, Pye CJ, Stone BJ (1978) A vibration technique for non-destructively assessing the integrity of structures. Journal of Mechanical Engineering Science 20(2):93–100.
- [2] Altunişik AC, Karahasan OŞ, Genç AF, Okur FY, Günaydin M, Kalkan E, Adanur S (2018) Modal parameter identification of RC frame under undamaged, damaged, repaired and strengthened conditions. Measurement 124:260–276.
- [3] Altunışık AC, Okur FY, Kahya V (2017) Modal parameter identification and vibration based damage detection of a multiple cracked cantilever beam. Engineering Failure Analysis 79:154–170.
- [4] An Y, Ou J (2012) Experimental and numerical studies on damage localization of simply supported beams based on curvature difference probability method of waveform fractal dimension. Journal of Intelligent Material Systems and Structures 23(4):415–426.
- [5] Bernal D, Levy A (2001) Damage localization in plates using DLVs. In: Proceedings of the 19th International Modal Analysis Conference. Orlando, FL.
- [6] Brincker R, Zhang L, Andersen P (2000) Modal identification from ambient responses using frequency domain decomposition. In: Proceedings of the 18th International Modal Analysis Conference (IMAC). San Antonio, Texas.
- [7] Brüel & Kjær Sound & Vibration Measurement (2021) BK Connect (Version 25.1) [Computer software]. B&K.
- [8] Brüel & Kjær Sound & Vibration Measurement (2021) PULSE Operational Modal Analysis (Version 7.1) [Computer software]. B&K.
- [9] Carrasco CJ, Osegueda RA, Ferregut CM, Grygier M (1997) Damage localization in a space truss model using modal strain energy. In: Proceedings–SPIE the International Society for Optical Engineering.
- [10] Cao M, Radzieński M, Xu W, Ostachowicz W (2014) Identification of multiple damage in beams based on robust curvature mode shapes. Mechanical Systems and Signal Processing 46(2):468–480.
- [11] Cawley P, Adams RD (1979) The location of defects in structures from measurements of natural frequencies. The Journal of Strain Analysis for Engineering Design 14(2):49–57.

- [12] Chang KC, Kim CW (2016) Modal-parameter identification and vibration-based damage detection of a damaged steel truss bridge. Engineering Structures 122:156–173.
- [13] Ciambella J, Vestroni F (2015) The use of modal curvatures for damage localization in beam-type structures. Journal of Sound and Vibration 340:126–137.
- [14] Computers and Structures Inc. (2021) SAP2000 (Version 21) [Computer software]. CSI. Available at: https://www.csiamerica.com.
- [15] Contursi T, Messina A, Williams EJ (1998) A multiple-damage location assurance criterion based on natural frequency changes. Journal of Vibration and Control 4(5):619–633.
- [16] Dai D, He Q (2014) Structure damage localization with ultrasonic guided waves based on a time-frequency method. Signal Processing 96:21–28.
- [17] Entezami A, Shariatmadar H (2018) An unsupervised learning approach by novel damage indices in structural health monitoring for damage localization and quantification. Structural Health Monitoring 17(2):325–345.
- [18] Fallah N, Vaez SRH, Mohammadzadeh A (2018) Multi-damage identification of large-scale truss structures using a two-step approach. Journal of Building Engineering 19:494–505.
- [19] Haynes C, Todd M (2015) Enhanced damage localization for complex structures through statistical modeling and sensor fusion. Mechanical Systems and Signal Processing 54:195–209.
- [20] Heylen W, Lammens S, Sas P (1997) Modal Analysis Theory and Testing. K.U. Leuven, Belgium.
- [21] Homaei F, Shojaee S, Amiri GG (2014) A direct damage detection method using multiple damage localization index based on mode shapes criterion. Structural Engineering and Mechanics 49(2):183–202.
- [22] Khatir S, Belaidi I, Khatir T, Hamrani A, Zhou YL, Wahab MA (2017) Multiple damage detection in composite beams using Particle Swarm Optimization and Genetic Algorithm. Mechanics 23(4):514–521.
- [23] Li H, Fang H, Hu SLJ (2007) Damage localization and severity estimate for three-dimensional frame structures. Journal of Sound and Vibration 301(3-5):481-494.
- [24] Li YY, Cheng L, Yam LH, Wong WO (2002) Identification of damage locations for plate-like structures using damage sensitive indices: strain modal approach. Computers & Structures 80(25):1881–1894.
- [25] Lu Q, Ren G, Zhao Y (2002) Multiple damage location with flexibility curvature and relative frequency change for beam structures. Journal of Sound and Vibration 253(5):1101–1114.
- [26] Nayyar A, Baneen U, Naqvi SA, Ahsan M (2021) Detection and localization of multiple small damages in beam. Advances in Mechanical Engineering 13(1):1687814020987329.
- [27] Park HS, Oh BK (2018) Damage detection of building structures under ambient excitation through the analysis of the relationship between the modal participation ratio and story stiffness. Journal of Sound and Vibration 418:122– 143.
- [28] Perez-Ramirez CA, Machorro-Lopez JM, Valtierra-Rodriguez M, Amezquita-Sanchez JP, Garcia-Perez A, Camarena-Martinez D, Romero-Troncoso RDJ (2020) Location of multiple damage types in a truss-type structure using multiple signal classification method and vibration signals. Mathematics 8(6):932.
- [29] Prajapat K, Ray-Chaudhuri S (2018) Detection of multiple damages employing best achievable eigenvectors under Bayesian inference. Journal of Sound and Vibration 422:237–263.
- [30] Reynders E, De Roeck G (2010) A local flexibility method for vibration-based damage localization and quantification. Journal of Sound and Vibration 329(12):2367–2383.
- [31] Rizos PF, Aspragathos N, Dimarogonas AD (1990) Identification of crack location and magnitude in a cantilever beam from the vibration modes. Journal of Sound and Vibration 138(3):381–388.
- [32] Sha G, Radzieński M, Cao M, Ostachowicz W (2019) A novel method for single and multiple damage detection in beams using relative natural frequency changes. Mechanical Systems and Signal Processing 132:335–352.
- [33] Shan S, Qiu J, Zhang C, Ji H, Cheng L (2016) Multi-damage localization on large complex structures through an extended delay-and-sum based method. Structural Health Monitoring 15(1):50–64.
- [34] Shi Z, Law SS, Zhang LM (1998) Structural damage localization from modal strain energy change. Journal of Sound and Vibration 218(5):825–844.
- [35] Stubbs N, Kim JT (1996) Damage localization in structures without baseline modal parameters. AIAA Journal 34(8):1644–1649.
- [36] Wu D, Law SS (2004) Damage localization in plate structures from uniform load surface curvature. Journal of Sound and Vibration 276(1–2):227–244.

[37] Xiang J, Liang M (2012) A two-step approach to multi-damage detection for plate structures. Engineering Fracture Mechanics 91:73–86.

- [38] Yang QW, Sun BX (2011) Structural damage localization and quantification using static test data. Structural Health Monitoring 10(4):381–389.
- [39] Yilmaz Z (2022) Numerical and Experimental Study of Damage Identification Using Modal Participation Ratio: Detection, Localization and Quantification of Several Damage Scenarios. MSc Thesis, Karadeniz Technical University.
- [40] Yilmaz Z, Okur FY, Günaydin M, Altunişik AC (2023) Enhanced modal participation ratio-based structural damage identification: A new filtering approach using modal assurance criteria. Buildings 13(10):2467.
- [41] Yuen MMF (1985) A numerical study of the eigenparameters of a damaged cantilever. Journal of Sound and Vibration 103(3):301–310.
- [42] Zhang S, Li CM, Ye W (2021) Damage localization in plate-like structures using time-varying feature and one-dimensional convolutional neural network. Mechanical Systems and Signal Processing 15(147):107107.
- [43] Zhuo D, Cao H (2022) Damage identification of bolt connection in steel truss structures by using sound signals. Structural Health Monitoring 21(2):501–517.